Leukemia (2019) 33:26–36
https://doi.org/10.1038/s41375-018-0165-2

ARTICLE

Acute myeloid leukemia

Profiling of aberrant DNA methylation in acute myeloid leukemia reveals subclasses of CG-rich regions with epigenetic or genetic association

Claudia Gebhard[1,2] · Dagmar Glatz[1,2] · Lucia Schwarzfischer[1] · Julia Wimmer[1] · Sebastian Stasik[3] · Margit Nuetzel[1] · Daniel Heudobler[1] · Reinhard Andreesen[1,2] · Gerhard Ehninger[3] · Christian Thiede[3] · Michael Rehli[1,2]

Received: 24 November 2017 / Revised: 19 March 2018 / Accepted: 24 April 2018 / Published online: 20 June 2018

Abstract

Malignant transformation is frequently associated with disease-specific epigenetic alterations, but the underlying mechanisms and pathophysiological consequences remain poorly understood. Here, we used global comparative DNA methylation profiling at CG-rich regions of 27 acute myeloid leukemia (AML) samples to select a subset of aberrantly methylated CG-rich regions (~400 regions, ~15,000 CpGs) for quantitative DNA methylation profiling in a large cohort of AML patients ($n = 196$) using MALDI-TOF analysis of bisulfite-treated DNA. Meta-analysis separated a subgroup of CG-rich regions showing highly correlated DNA methylation changes that were marked by histone H3 lysine 27 trimethylation in normal hematopoietic progenitor cells. While the group of non-polycomb group (PcG) target regions displayed methylation patterns that correlated well with molecular and cytogenetic markers, PcG target regions displayed a much weaker association with genetic features. However, the degree of methylation gain across the latter panel showed significant correlation with active DNMT3A levels and with overall survival. Our study suggests that both epigenetic as well as genetic aberrations underlay AML-related changes in DNA methylation at CG-rich regions and that the former may provide a marker to improve classification and prognostication of adult AML patients.

Introduction

Acute myeloid leukemia (AML) is the most common type of acute leukemia in adults and a highly heterogeneous and fatal disease. Despite recent progress in classifying AML patients according to cytogenetic and molecular markers, genetic risk groups still do not live up to the heterogeneity of the disease. Currently, patients are grouped into low, intermediate, or high risk based on cytogenetic data [1–5]. For the largest and highly heterogeneous group of AML patients with normal karyotype (NK-AML), specific genetic alterations of *NPM1*, *CEBPA*, *FLT3*, *KIT*, *DNMT3A*, *IDH1/2*, *WT1*, or *MLL* genes appear to be clinically relevant, but the current classification system is still insufficient [6–12].

In addition to genetic aberrations, disease-related epigenetic changes may reflect biological processes that are also relevant for disease progression, treatment response, or outcome. Early studies have highlighted an abundance of epigenetic alterations in various types of cancer, including AML [13–17]. A commonly observed alteration is the aberrant (but potentially therapeutically reversible) DNA methylation that can target tumor suppressor genes and may have a role in disease pathogenesis [18].

The exact mechanisms shaping disease-specific DNA methylation signatures are still poorly understood, but likely involve multiple distinct events that can be sequence-dependent or -independent, targeted or random, which are then selected for during clonal evolution, either as a passenger, or driver.

Electronic supplementary material The online version of this article (https://doi.org/10.1038/s41375-018-0165-2) contains supplementary material, which is available to authorized users.

✉ Michael Rehli
michael.rehli@ukr.de

[1] Department of Internal Medicine III, University Hospital Regensburg, 93042 Regensburg, Germany

[2] RCI Regensburg Centre for Interventional Immunology, University Hospital Regensburg, 93042 Regensburg, Germany

[3] Department of Internal Medicine I, University Hospital Carl Gustav Carus, 01307 Dresden, Germany

Several recent AML profiling studies provided clear evidence for the presence of distinct DNA methylation signatures associated with specifically altered transcriptional regulators, including several oncofusion proteins (RUNX1-RUNX1T1, CMFß-MYH11, PML-RARA), mutated transcription factors (TFs) like CEBPA or RUNX1, the mutated phosphoprotein NPM1, or the deregulated transcription factor EVI1 [19–22]. In some cases, oncogenetic TFs (like the RUNX1-RUNX1T1 protein) may recruit DNMTs to their target sites leading to abnormal DNA methylation patterns [23]. In other cases, the methylation state may inversely correlate with TF binding. Previous work has shown that hematopoietic TFs (like CEBPA) as well as a number of general transcription factors (like Sp1, GABP, YY1), share a methylation-protective role since their binding and de novo DNA methylation are mutually exclusive [24–26]. More generally, TFs may be responsible for establishing and maintaining hypermethylated states [27]. Alterations of transcription factor networks may thus have a marked impact on the development of disease-specific epigenetic signatures at specific *cis*-elements. In addition to locally acting TFs, several recurrent mutations in epigenetic regulators were identified with the potential to affect DNA methylation patterns globally. These include mutations in additional sex combs-like 1 (*ASXL1*) [28], in DNA-methyltransferase 3A (*DNMT3A*) [9] as well as their recruitment to methylation targets by deregulated or mutated epigenetic modifiers like histone methyltransferases G9a [29, 30] or the enhancer of zeste homologue 2 (*EZH2*) [31]. Other frequently mutated epigenetic regulators include tet methylcytosine dioxygenase 2 (*TET2*), which has been implicated in DNA demethylation, or isocitrate dehydrogenases (*IDH1/2*), which produce the oncometabolite 2-hydroxyglutarate (2-HG), which inhibits α-ketoglutarate-dependent dioxygenases (like TET2) [10, 19, 32, 33].

Altered DNA methylation patterns in cancer are predominantly found at CpG-dense regions, which include the so-called CpG islands (CGI). In contrast to many CpG-sparse *cis*-regulatory modules, the vast majority of CG-rich regions is unmethylated in normal somatic tissues at both active and repressed genes (with the exception of imprinted loci, the inactive X chromosome of females and few tissue-specific regulatory regions) and their methylation status does not correlate with tissue-specific gene expression [34, 35]. Notably, many CG-rich regions that are de novo DNA methylated in cancer are targets of PcG repression and marked by histone H3 lysine 27 trimethylation (H3K27me3) in embryonic stem cells [36]. Although this association is clearly evident from several studies, the mechanistic basis for this phenomenon is still unclear [37–39].

The quantitative DNA methylation profiling of CG-rich regions performed in this study suggests that DNA methylation alterations are either linked with previous PcG repression in normal hematopoietic progenitor cells (HPC) or associated with specific genetic lesions. Aberrant DNA methylation at non-PcG target regions segregates patients into specific AML subgroups with prominent biological differences, while the gain of DNA methylation at CG-rich regions that are targeted by PcG in HPC is linked with higher levels of active DNMT3A and may be of prognostic relevance in AML.

Material and methods

DNA preparation from normal cells and clinical samples

All clinical samples were derived from patients enrolled into the AML96 protocol of the Study Alliance Leukemia (SAL). Leukemic blasts and bone marrow cells from AML patients were collected during routine diagnostic bone marrow aspirations. All patients had given informed consent to additional sample collection and analyses according to a protocol approved by the local ethical committee.

The clinical data have been published previously [40] and are summarized in Supplementary Table S1. Human peripheral blood monocytes from several healthy donors (male, age 20–60) were purified from PBMCs by elutriation or CD14-selection. To isolate human neutrophils from peripheral blood an ACK lysis was performed prior to FACS sorting. Human HPC cells were purified as described elsewhere [41]. Briefly, leukapheresis products obtained from normal individuals were used and cell populations expressing mature erythroid, granulopoietic, megakaryopoietic and lymphoid markers were removed using a StemSep column (StemCell Technologies Inc., Vancouver, BC) resulting in a Lin^- cell fraction comprising 84 ± 10% CD34+ cells. Lin^- cells were incubated with anti-human CD34-APC (8G12, Becton–Dickinson, St. Jose´, CA, USA), CD38-PE (HB-7, Becton–Dickinson) and CD45-FITC (Dianova, Hants, UK) and cell sorting was done on a FACStarPlus (Becton–Dickinson). DNA from hematopoietic cell types was prepared using the Qiagen Blood & Cell Culture DNA Kit. DNA concentration was determined with the NanoDrop spectrophotometer and quality was assessed by agarose gel electrophoresis.

Mass spectrometry analysis of bisulfite-converted DNA

For quantitative analyses of aberrantly methylated CG-rich regions in a larger patient cohort, we selected a total of 384 differentially methylated regions (DMR), based on criteria outlined in the Supplementary Methods online. The set of 384 CpG island regions (listed in

Supplementary Table S2) was analyzed by MALDI-TOF MS of bisulfite-converted DNA [42]. Genomic sequences of selected regions were extracted from the UCSC genome browser (www.genome.ucsc.edu/). PCR primers were designed using Methprimer (www.urogene.org/methprimer/) and sequences are provided in Supplementary Table S2. Sodium bisulfite conversion was performed using EZ DNA methylation kit (Zymo Research, California, USA) using 1 µg of genomic DNA and an alternative conversion protocol (elution with water instead of M-Elution buffer; cycler conditions: 95°C for 30 s, 50°C for 15 min, 20 cycles). The amplification of target regions was followed by SAP treatment, reverse transcription and subsequent RNA base-specific cleavage (MassCLEAVE, Agena, San Diego, CA) as previously described [42]. Cleavage products were loaded onto silicon chips (spectroCHIP, Agena, San Diego, CA) and analyzed by MALDI-TOF mass spectrometry (MassARRAY Compact MALDI-TOF, Agena, San Diego, CA). Methylation was quantified from mass spectra using the Epityper software v1.0 (Agena, San Diego, CA) and results for 196 patients as well as 15 control samples are provided in Supplementary Table S3.

Analysis of quantitative DNA methylation data

We initially assigned mean methylation ratios to regions covered by individual Epityper amplicons based on all measured CpGs within the regions. Eighty-four regions were filtered for quality of spectra, variance, and redundancy as outlined in the Supplementary Methods. For the remaining set of 300 regions, we calculated and clustered a Pearson correlation matrix (in *R* environment). Annotation of epigenetic data sets (listed in Supplementary Table S4) to individual regions was done using HOMER. Histograms were visualized using *R*. Hierarchical clustering of patients and region subsets was also performed in *R*. Graph-based clustering was performed and visualized using BiolayoutExpress^{3D}. Survival analysis was performed using the package survival in *R*. To separate patients into high and low methylation groups we ranked them by their averaged methylation ratios across PcG target regions and split them into two groups comprising equal cumulative methylation ratios. Computer code is available upon request.

Mutation analysis using PCR

Molecular alterations in Nucleophosmin 1 (*NPM1*) exon 12, *FLT3* exons 14 and 15, *CEBPA* and IDH1 and IDH2 exons 4 were characterized as published in detail previously [43–46]. Mutational analysis for *NRAS, KRAS, CBL, TET2, EZH2, ASXL1, WT1*, and *KIT* (D816V) were performed by MLL, Munich. Coding exons of *PHF6* were PCR-amplified from genomic DNA with primer sequences given in Supplementary Table S5. Sequence analysis was carried out by conventional Sanger sequencing (Geneart, Regensburg, Germany).

Mutation profiling of a target panel using NGS

Mutation profiling of genes frequently mutated in AML was done by targeted resequencing using the TruSight Myeloid assay (Illumina, Chesterford, UK) which covers the entire coding region or mutational hotspots of the following 54 genes: BCOR, BCORL1, CDKN2A, CEBPA, CUX1, DNMT3A, ETV6, EZH2, IKZF1,KDM6A, PHF6, RAD21, RUNX1, STAG2, and ZRSR2 and oncogenic hotspots of ABL1, ASXL1, ATRX, BRAF, CALR, CBL, CBLB, CBLC, CDKN2A, CSF3R, FBXW7, FLT3, GATA1, GATA2, GNAS, HRAS, IDH1, IDH2, JAK2, JAK3, KIT, KRAS, MLL, MPL, MYD88, NOTCH1, NPM1, NRAS, PDGFRA, PTEN, PTPN11, SETBP1, SF3B1, SMC1A, SMC3, SRSF2, TET2, TP53, U2AF1, and WT1. For the analysis, 50 ng of genomic DNA were use, library preparation was done as recommended by the manufacturer (TruSight Myeloid Sequencing Panel Reference Guide 15054779 v02, Illumina). Samples were paired-end sequenced (2 × 225 bp) on a MiSeq NGS-instrument using V3-chemistry (Illumina). Sequence data alignment of demultiplexed FastQ files, variant calling and filtering was done using the Sequence Pilot software package (JSI medical systems GmbH, Ettenheim, Germany) with default settings and a 5% variant allele frequency (VAF) mutation calling cut-off. Detection of large insertions was performed using PINDEL algorithm3 following BWA-MEM2 mapping with default settings. Human genome build HG19 was used as reference genome for mapping algorithms.

Statistical analysis

Enrichment of patient features in DNA methylation clusters was analyzed using Fisher's exact test. Correction for multiple testing was done according to Benjamini–Hochberg applying a false discovery rate (FDR) of 5%. Analyses of patient survival using Cox proportional-hazards regression and Kaplan–Maier estimation were done using the package survival in *R* (http://cran.r-project.org/package=survival).

Results

Genome-wide comparative DNA methylation profiles of normal and AML cells

To globally define AML-related DNA methylation aberrations we initially profiled a representative set of 27 AML samples for aberrant DNA methylation using our previously

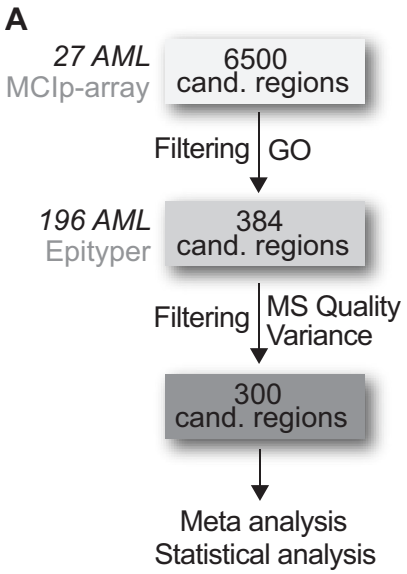

B

Summary of clinical data for the 195 AML patients studied.

Gender:		***Karyotype:***	
Male	104	Normal	94
Female	91	Aberrant	95
		inv(16)	18
Age:		t(8;21)	5
<60 years	112	del5(q)	10
>60 years	83	del7(q)	17
FAB:		***Molecular Markers:***	
M0	13	FLT3	64
M1	40	NPM1	54
M2	51	DNMT3A	49
M4	20	TET2	47
M4E0	17	IDH1/2	37
M5	1	CEBPA	27
M5a	38	RUNX1	25
M5b	9	NRAS	23
M6	2	ASXL1	22
RAEB	1	GATA2	16
RAEB-T	2	RAD21	15

Fig. 1 Workflow for the quantitative methylation profiling and clinical data of the AML cohort. **a** From the large set of CG-rich regions displaying altered DNA methylation patterns in AML patients, 384 regions were selected for fine mapping in a larger cohort of 196 AML patients. After quality controlling and filtering for variability between normal samples from healthy donors, a subset of 300 CG-rich regions were used for meta- and statistical analyses. **b** Overview of the clinical data for the 196 patients. We did not include M3 patients because they are known to represent a separate disease entity

described methyl-CpG immunoprecipitation (MCIp) technique combined with microarray hybridization (see Supplementary text for details) [26, 47–49]. Comparative DNA methylation profiles across 23,000 CpG-rich regions identified > 6,500 regions altered in at least three patients (Supplementary Figure S1). To investigate the relationship of altered DNA methylation patterns and clinical/molecular features in a larger patient cohort, we decided to focus on differentially methylated, autosomal candidate CG-rich regions in close vicinity to genes with known functions during myelopoiesis as well as genes generally associated with gene regulatory processes (see Supplementary Methods) and selected 384 candidate CG-rich regions (covering > 15,000 individual CpG dinucleotides) for quantitative DNA methylation measurement (bisulfite conversion and subsequent MALDI-TOF MS analysis) [42].

The workflow as well as clinical data of the AML patient cohort is outlined in Fig. 1. Along with 196 AML patient samples we measured methylation ratios of several normal control samples including three CD34+ progenitor cell samples, as well as two CD15+ granulocyte samples and fifteen CD14+ monocyte samples (four donors age < 30 years; eleven donors age > 59 years).

The original set of 384 differentially methylated candidate CG-rich regions was filtered according to the spectral quality from the MALDI-TOF MS output, amplification bias and variability across samples. After removing regions with low quality, little variance between AML or high variability in controls (which frequently correlated with either local genotype, age or gender, Supplementary Figure S2), a set of 300 CG-rich regions remained that showed stable DNA methylation profiles across controls, independent of differentiation stage, age and gender.

Aberrant DNA methylation segregates CG-rich regions into clusters with distinct epigenetic signatures in HPC

Since correlated changes across patients between differentially methylated candidate regions could indicate a mechanistic linkage, we studied similarities between aberrantly methylated regions by generating a hierarchically clustered Pearson correlation matrix. Clustering of the correlation matrix including DNA methylation ratios of the 300 CG-rich target regions across 196 AML patients clearly separated CG-dense regions into two distinct clusters (Fig. 2). To further characterize differentially methylated candidate regions, we also annotated publicly available epigenetic data sets for normal human CD34+ hematopoietic progenitor (HPC) and embryonic stem cells (ESC). As shown in Fig. 2 the two main clusters were already pre-marked by distinct epigenetic profiles in healthy HPC and (to a lesser extent) in ESC. In particular, the lower cluster showed highly correlated DNA methylation changes across all patient samples, and mainly comprises PcG targets (marked by trimethylation of lysine 27 on histone H3 [H3K27me3]) in HPC (PcG cluster). In contrast, the top cluster showed low levels of H3K27me3 in HPC as well as a clear enrichment of H3K27ac, H3K4me3 and DNase-I hypersensitivity compared to the bottom cluster in HPC (Fig. 2, nPcG cluster). The highly correlated methylation pattern of the PcG cluster suggests a common mechanistic basis for DNA methylation changes at these differentially methylated candidate regions.

To validate the linkage between epigenetic signatures in HPC and highly correlated DNA methylation clusters with

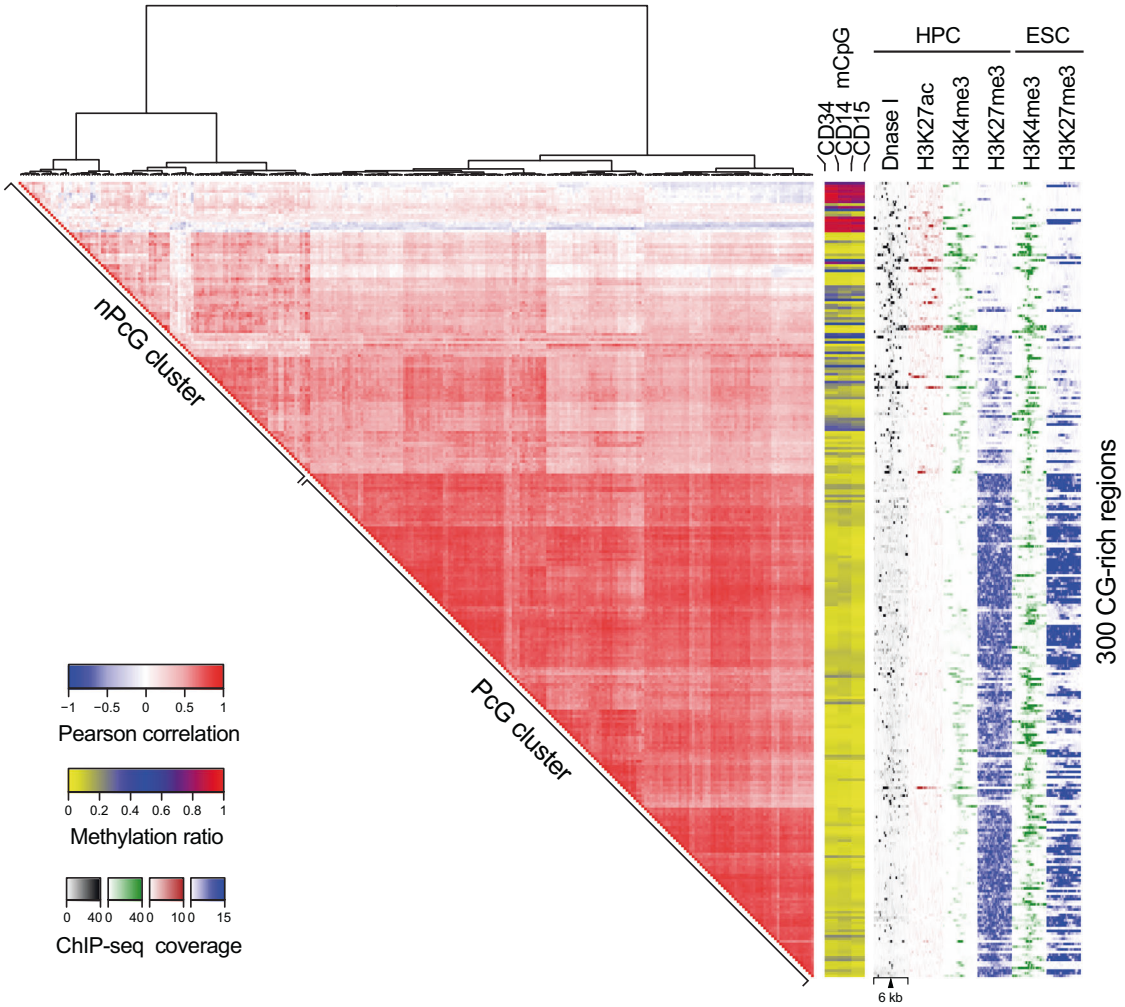

Fig. 2 Aberrant DNA methylation in AML segregates epigenetically distinct CG-rich regions in normal hematopoietic progenitor cells. Heatmap representation of the hierarchically clustered Pearson correlation matrix of DNA methylation ratios for the 300 selected CG-rich regions across 196 patients. Correlation data are shown along with DNA methylation ratios for normal cell types (CD34, HPC; CD14, monocytes; CD15, granulocytes) as well as histograms for genomic distance distributions of DNase-I-seq and the indicated ChIP-seq tag counts of CD34+ hematopoietic progenitor cells (HPC) and embryonic stem cells (ESC) centered across CG-rich regions across a 6 kb genomic region. The bottom cluster showing the strongest correlation of CGI DNA methylation data across patients is highly enriched for H3K27me3, particularly in HPC (PcG cluster), while the upper cluster is not associated with H3K27me3 (nPcG cluster)

an independent data set, we performed a similar unsupervised Pearson correlation based clustering with 450 K Illumina Bead Array DNA methylation data from The Cancer Genome Atlas (TCGA) [21]. Analysis of DNA methylation ratios of CG-rich regions across ~200 AML patients again identified a highly correlated group of hypermethylated regions that represent PcG target genes in HPC (Supplementary Figure S3). Major DNA methylation clusters generally correlated with epigenetic states in HPC, suggesting that the susceptibility of many CG-rich regions for DNA methylation changes during leukemic transformation is already imprinted in normal progenitor cells (Supplementary Figure S3). Individual clusters were also characterized by distinct sequence motif signatures (Supplementary Figure S3) as described previously [26].

Non-PcG targets segregate patients into clusters with genetic association

Based on the results above we then asked how methylation patterns of PcG and nPcG clusters correlated across patients. Taking a pair-wise Pearson correlation matrix of the methylation profiles in each cluster, we used the Markov Cluster (MCL) algorithm [50] to group patients that share similar methylation profiles across the cohort. Figure 3 and Supplementary Figure S4 show graphical overviews of the MCL-clustered data for the nPcG cluster regions. Visualization of the correlation matrix with $r > 0.6$ grouped all patients into a single component and MCL separated two clusters, with the small one including only five patients (Fig. 3a). These patients (all classified as immature M0/M1

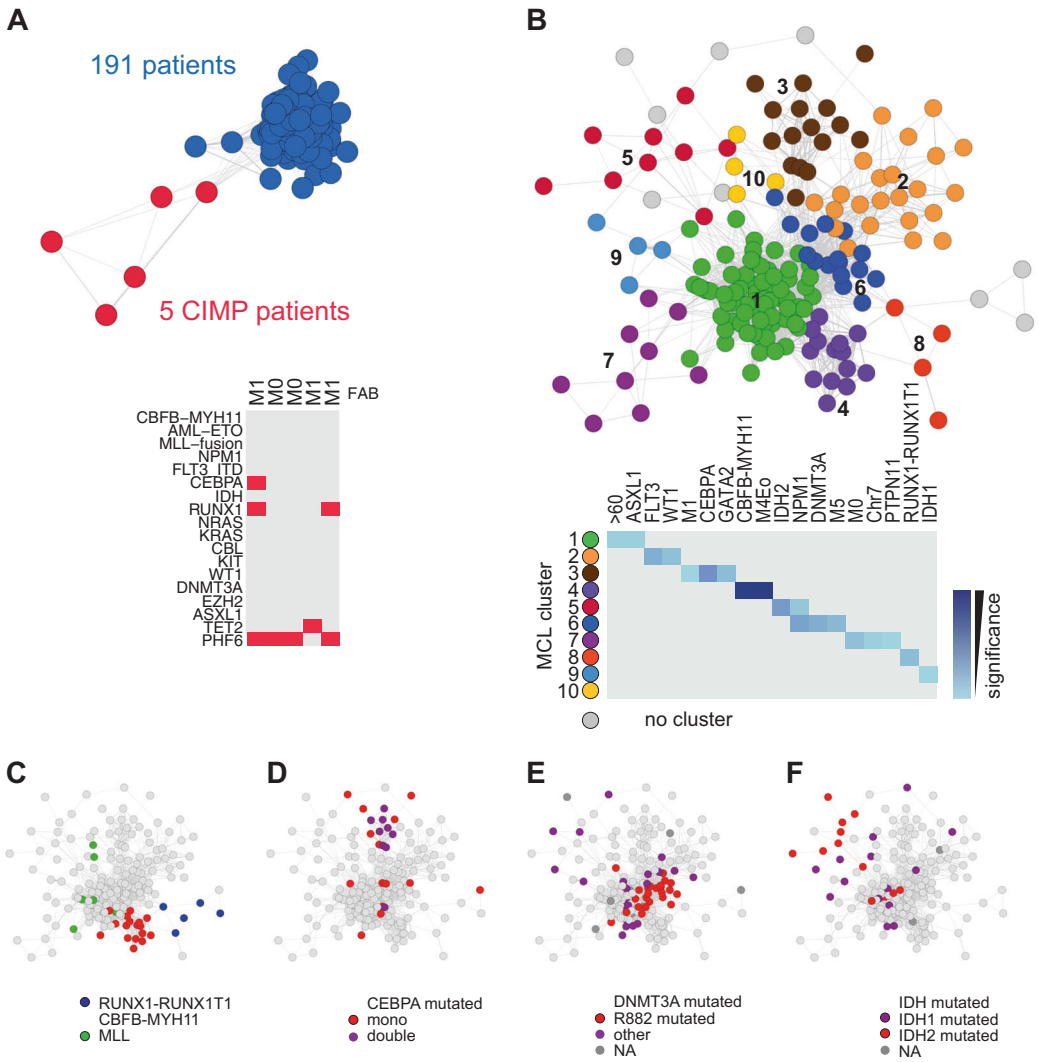

Fig. 3 Non-PcG targets segregate patients into clusters with genetic association. **a** Co-clustering network based on Pearson correlations between DNA methylation profiles across non-PcG target regions of all AML patients at a correlation of $r > 0.6$. The cluster network was visualized using BiolayoutExpress[3D]. MCL clustering (MCLi = 2.2) identified two clusters (indicated by coloring). The heatmap below the graph indicates the mutational status of the separate group of highly methylated CIMP patients along with their FAB classification. **b** Co-clustering network based on Pearson correlations between DNA methylation profiles across non-PcG target regions of 191 AML patients that were included into the major component at a correlation of $r > 0.75$. The cluster network is visualized using BiolayoutExpress[3D] and clusters of correlated patients (MCLi = 2.2) are indicated by coloring. The heatmap below the graph indicates significant associations ($P < 0.05$, Benjamini–Hochberg corrected Fisher's exact test) with FAB clusters, age, or the indicated genetic features. **c–f** Color-coded visualization of patient genetic features within the co-clustering network shown in **b**. Additional features are shown in Supplementary Figure S4

AML) displayed a concerted hypermethylation at the large majority of studied loci and represent a rare extreme CGI methylator phenotype (CIMP) in AML. Since these five patients showed very few and no recurrent mutations in the original gene panel (*NPM*, *FLT3-ITD*, *CEBPA*, *IDH1/2*, *RUNX*), we sequenced additional candidate genes that were previously implicated in AML and could potentially explain the extreme hypermethylation phenotype (including *NRAS, KRAS, CBL, KIT, WT1, DNMT3A, EZH2, ASXL1, TET2*, and *PHF6*). Strikingly, only PHF6 was found mutated in 4 out of the 5 hypermethylated patients (Fig. 3a), while none of the other candidate genes were recurrently mutated in these patients. The underlying cause for the extreme hypermethylation signature remains unclear and is subject to ongoing studies.

MCL clustering of the nPcG cluster correlation matrix with a more stringent correlation cut-off ($r > 0.75$) segregated patients into 10 distinct clusters (MCL cluster 1–10, indicated by coloring) (Fig. 3b). The clustering results indicated the association of most methylation-based patient clusters with molecular and genetic markers (Fig. 3c–f, and Supplementary Figure S4). Two patient clusters were

significantly associated with the presence of oncofusion proteins, including CBFB-MYH11 (cluster 4, $P < 1.2 \times 10^{-15}$, Fisher's exact test, Benjamini–Hochberg multiple testing correction) and RUNX1-RUNX1T1 (cluster 8, $P < 0.0025$). Other clusters were clearly enriched for mutations in *CEBPA* (cluster 3, $P < 2.6 \times 10^{-6}$), *GATA2* (cluster 3, $P < 0.0025$). *IDH1* (cluster 9, $P < 0.05$), *IDH2* (cluster 5, $P < 1.5 \times 10^{-5}$), *NPM1* (cluster 6, $P < 4 \times 10^{-5}$), *DNMT3A* (cluster 6, $P < 0.0002$), *FLT3* (cluster 2, $P < 0.00025$), *WT1* (cluster 2, $P < 0.0035$), *ASXL1* (cluster 1, $P < 0.05$), *PTPN11* (cluster 7, $P < 0.05$), or deletions of chromosome 7 (cluster 7, $P < 0.05$). Some clusters also showed significant associations with patients' FAB classification or age (Fig. 3b). In contrast, MCL clustering of the larger set of the PcG cluster regions did not reveal separate clusters across patients. We also used unsupervised two-dimensional hierarchical clustering to group patients according to methylation profiles in PcG and nPcG cluster regions (Supplementary Figure S5). In line with the MCL approach, hierarchical clustering of the nPcG cluster regions grouped samples into clusters showing highly significant correlation with genetic markers. In contrast, PcG cluster regions resulted in fewer patient clusters showing less correlation with genetic markers. As also observed with the MCL approach, CIMP patients formed separate groups (PHF6 group), both in the PcG and nPcG cluster setting (Supplementary Figure S5). Similar observations were also made for clusters derived from TCGA data. Again, clusters associated with aberrant DNA methylation and pre-marked with H3K27me3 in HPC correlated less with molecular and genetic markers than the nPcG clusters (Supplementary Figure S6).

High methylation levels at PcG target genes were associated with active DNMT3A levels and a better survival

DNA methylation at PcG cluster regions more or less resembled a continuous range of methylation levels (Fig. 4a). Since aberrant DNA methylation at PcG cluster loci did not show a clear correlation with cytogenetic or molecular markers, we explored its possible value as prognostic marker in AML. Kaplan–Meier survival curves showed a significant difference in overall survival between patients with high or low average levels of DNA methylation across PcG cluster regions. Interestingly, higher methylation levels at PcG cluster regions were associated with a better prognosis ($P < 0.01$; log-rank test) (Fig. 4b). We also found an enrichment of more immature (FAB M1), *WT1* or *CEBPA* mutated AMLs in this group, while lower methylation levels were significantly associated with *DNMT3A* mutations and more mature AMLs (FAB M5) (Fig. 4c). Since *DNMT3A* mutations have previously been associated with a worse prognosis [9, 51], and may directly impact on DNA methylation levels, we specifically tested Cox proportional hazard models including both *DNMTA3* mutation status and association with either high or low methylation, and both sequential testing or tests for interaction revealed no impact of the *DNMT3A* mutation status on overall survival in our cohort, while the high DNA methylation level group was significantly associated with a better survival. To evaluate whether this methylation prediction model can also be applied to an independent patient set, we performed a comparable analysis using the TCGA DNA methylation data (Supplementary Figure S7A) [21]. Univariate analysis again revealed a significantly better survival of patients within the high PcG cluster CGI methylation group ($P < 0.05$; log-rank test) (Supplementary Figure S7B). The frequency distribution of patient characteristics for high and low DNA methylation groups resembled the one from our cohort (Fig. 4c, lower panel). Analysis of TCGA AML mRNA expression data showed that there is also a clear difference in *DNMT3A* mRNA expression levels, even in *DNMT3A* wild-type patients (Fig. 4d), suggesting that low DNA methylation levels (associated with poor survival) are associated with less active DNMT3A (either due to transcriptional down-regulation or due to loss of function mutation).

To evaluate the relative impact of the quantitative DNA methylation levels on the outcome of patients we then performed a Cox proportional hazard analysis considering age (<60, ≥60), *TP53* and *BCORL1* mutation status, presence of *CBFB-MYH11* fusion, or whole blood cell counts above 100 per microliter in the model, which were identified as significantly associated with overall survival in univariate analyses. As shown in Table 1 and Supplementary Figure S7C, in a multivariate analysis, high levels of DNA methylation at PcG-cluster regions were not independently associated with a better survival in either cohort.

To validate the difference in *DNMT3A* mRNA expression levels in our cohort, we studied gene expression in a subset of patients using quantitative RT-PCR. As shown in Supplementary Figure S8 the difference in DNMT3A expression was significant and comparable to the TCGA cohort.

Discussion

Altered DNA methylation landscapes are a common feature of cancers, including leukemia, and are known for several decades. The underlying mechanisms, however, are not well understood. In the present study, we analyzed alterations in CG-rich DNA methylation patterns in AML, and identified two independent groups of alterations that are likely driven by different mechanisms. The first one is associated with PcG

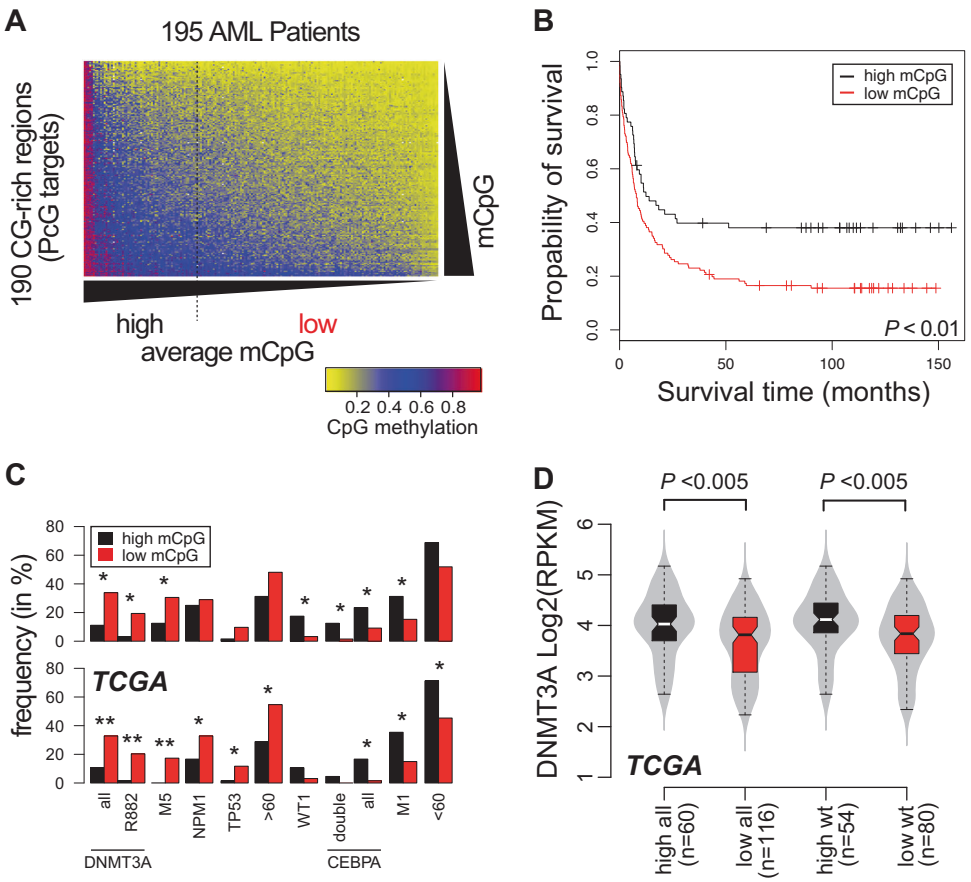

Fig. 4 Survival analysis based on average PcG target methylation levels. **a** Heatmap representation of DNA methylation patterns sorted by mean methylation ratios across patients and PcG cluster CG-rich regions. High and low DNA methylation groups of patients were divided at a mean methylation ratio of 0.28 based on equal cumulative methylation levels within each group. **b** Kaplan–Meier survival analysis with the high (black line) and low (red line) DNA methylation (mCpG) group showing a significant difference in overall survival ($P < 0.01$; log-rank test). **c** Barplot of mutation frequencies for genes showing significant enrichment in either low or high mCpG group. Significance is indicated by asterisks (***$P < 0.001$, **$P < 0.01$, *$P < 0.05$, Fisher's exact test). The upper panel represents the AML cohort of this study, while the lower panel corresponds to TCGA AML data. **d** Combined bean and boxplot showing the distribution of DNMT3A expression values (RPKM) across TCGA AML patients in the low or high mCpG group ($P < 0.005$; Wilcox test)

Table 1 Results of multivariate analysis

	HR	Lower CI	Upper CI	*P*
PcG target mCpG	2.03	1.62	2.84	n.s. (0.08)
Age (<60, ≥60)	9.49	4.77	25.58	<0.001
TP53 mutation	7.79	2.92	50.77	<0.05
CBFB-MYH11 fusion	1.88	1.35	3.74	n.s. (0.22)
BCORL1 mutation	14.09	4.43	109.89	<0.001
WBC>100	9.50	4.29	32.53	<0.001

repression in HPC, common to all AML samples (and likely due to a single mechanism) and independently relevant for prognosis. Here the DNA methylation levels at least partially depend on active DNMT3A levels (either regulated transcriptionally or altered by mutation). The second group comprises CG-rich regions displaying both disease-specific hypo- and hypermethylation events that show a strong correlation with genetic lesions, are specific to individual patients and likely involve multiple mechanisms (depending on the genetic alteration). These results shed new light on the formation of complex methylation patterns during leukemogenesis and are in line and extend previous work on DNA methylation patterns in AML [37, 52–54].

The quantitative DNA methylation data of 300 selected CG-rich regions across 196 AML patients clearly segregates those regions into two major clusters. The most highly correlated cluster contains CG-rich loci that acquire DNA methylation during leukemogenesis and are almost always targets of PcG repressors in HPC (and to a lesser degree already in ESC). The correlation between PcG repression in ESC and aberrant DNA methylation has previously been observed in many types of cancer, including AML [36, 53, 55–59]. Our meta-analysis of epigenetic data for HPC suggests, that the link between aberrant methylation of CG-rich regions and PcG repression is even stronger for the

lineage-matched progenitor cell. Epigenomic data sets from matched normal progenitor cells (in particular the histone modification H3K27me3) may thus generally be helpful to classify aberrant methylation of CG-rich regions in various types of cancer. This finding further supports the hypothesis that reversibly active *cis*-regulatory modules in stem or progenitor cells are permanently silenced in cancer cells with a perpetual state of self-renewal [59]. Furthermore, earlier studies have described a direct connection between EZH2 and the DNMTs [60], thus providing a possible mechanism for DNA methylation at PcG targets during cancer development.

Methylation classifiers predicting AML outcome have been published previously [54, 61], however, the underlying biology is unclear. In the present study, outcome is linked with biology, namely the epigenetic state of regions in progenitor cells. In line with a previous report [37], the overall degree of methylation at CG-rich PcG cluster regions represents an independent prognostic factor for patient survival. Interestingly, patients displaying high methylation levels at PcG cluster loci showed a significant better survival than patients with lower levels of DNA methylation at these CG-rich regions. One possible explanation of the observed inverse correlation may be related to the link between cellular aging and aberrant methylation of the PcG cluster regions. Since age-dependent differences likely reflect a higher mitotic age, aberrant methylation at PcG cluster loci could correlate with higher mitotic activities of leukemia cells, which may improve the success of standard chemotherapy. Another possible explanation is the enrichment of *CEBPA* mutations in the patient group with high DNA methylation while lower levels of active DNMT3A (either by mutation or transcriptional downregulation) are found in the patient group with low DNA methylation level. It is known that patients harboring *CEBPA* mutations show better overall survival [7, 12, 62–68], while *DNMT3A* mutations correlate with worse prognosis [9, 51].

In contrast to the PcG target regions, the remaining CG-rich regions (nPcG cluster) showed a strong association with (cyto)genetic and molecular aberrations. This observation is in line with earlier findings by others [37, 52–54, 69] and suggests that most changes at these CG-rich regions (both gains and losses of DNA methylation) are directly related to the genetically altered transcriptional networks in AML patients.

Previous studies established a link between mutations in the demethylation pathway (IDH1/2 or TET2) and pronounced hypermethylation [19, 20]. Interestingly, neither *IDH1/2* nor *TET2* mutations were preferentially associated with high methylation PcG cluster group regions. Instead, the patient cluster associated with *IDH* mutations within the nPcG cluster contained highly methylated samples. However, the highest degree of methylation is detected in five patients with immature (M0/1) and mixed leukemia (with coexpression of myeloid and lymphoid markers) which form separate clusters in both PcG and nPcG cluster regions (see Fig. 3a and Supplementary Figure S5) and share *PHF6* mutations in four out of five patients. This phenotype is not explained by *IDH* nor *TET2* mutations and may resemble a subgroup of biphenotypic AMLs described earlier [70, 71]. The exact molecular mechanism causing this CGI hypermethylation phenotype (CIMP) in AML is unclear. However, this patient subgroup may particularly benefit from therapies including demethylating agents.

In conclusion our studies reveal that CG-rich regions showing aberrant methylation in AML basically fall into two categories: (1) A large group of commonly altered CG-rich regions that are already marked by PcG repressors in normal HPC and poised to acquire DNA methylation and (2) CG-rich regions that are altered due to the genetically altered transcriptional landscape in AML. Both categories provide independent information and should be considered separately in future studies.

Acknowledgements We thank Johanna Raithel for excellent technical assistance. This work was funded by grants from the Wilhelm Sander Foundation and the German Cancer Aid to MR.

Author contributions CG, RA, and MR designed research; CG, DG, LS, JW, SS, DH, and MN performed research; GE and CT contributed clinical samples, new reagents, or analytic tools; CG and MR analyzed data; CG and MR wrote the paper.

Conflict of interest CT is part owner and CEO of AgenDix GmbH. The remaining authors declare that they have no conflict of interest.

References

1. Byrd JC, Mrozek K, Dodge RK, Carroll AJ, Edwards CG, Arthur DC, et al. Pretreatment cytogenetic abnormalities are predictive of induction success, cumulative incidence of relapse, and overall survival in adult patients with de novo acute myeloid leukemia: results from Cancer and Leukemia Group B (CALGB 8461). Blood. 2002;100:4325–36.
2. Grimwade D, Walker H, Oliver F, Wheatley K, Harrison C, Harrison G, et al. The importance of diagnostic cytogenetics on outcome in AML: analysis of 1,612 patients entered into the MRC AML 10 trial. The Medical Research Council Adult and Children's Leukaemia Working Parties. Blood. 1998;92:2322–33.
3. Mrozek K, Heerema NA, Bloomfield CD. Cytogenetics in acute leukemia. Blood Rev. 2004;18:115–36.
4. Slovak ML, Kopecky KJ, Cassileth PA, Harrington DH, Theil KS, Mohamed A, et al. Karyotypic analysis predicts outcome of preremission and post remission therapy in adult acute myeloid leukemia: a Southwest Oncology Group/Eastern Cooperative Oncology Group Study. Blood. 2000;96:4075–83.
5. Rowley JD. Chromosomal translocations: revisited yet again. Blood. 2008;112:2183–9.
6. Bacher U, Schnittger S, Haferlach T. Molecular genetics in acute myeloid leukemia. Curr Opin Oncol. 2010;22:646–55.
7. Dohner H, Estey EH, Amadori S, Appelbaum FR, Buchner T, Burnett AK, et al. Diagnosis and management of acute myeloid

leukemia in adults: recommendations from an international expert panel, on behalf of the European LeukemiaNet. Blood. 2010;115:453–74.
8. Hou HA, Huang TC, Lin LI, Liu CY, Chen CY, Chou WC, et al. WT1 mutation in 470 adult patients with acute myeloid leukemia: stability during disease evolution and implication of its incorporation into a survival scoring system. Blood. 2010;115:5222–31.
9. Ley TJ, Ding L, Walter MJ, McLellan MD, Lamprecht T, Larson DE, et al. DNMT3A mutations in acute myeloid leukemia. N Eng J Med. 2010;363:2424–33.
10. Mardis ER, Ding L, Dooling DJ, Larson DE, McLellan MD, Chen K, et al. Recurring mutations found by sequencing an acute myeloid leukemia genome. N Eng J Med. 2009;361:1058–66.
11. Patel JP, Gonen M, Figueroa ME, Fernandez H, Sun Z, Racevskis J, et al. Prognostic relevance of integrated genetic profiling in acute myeloid leukemia. N Eng J Med. 2012;366:1079–89.
12. Schlenk RF, Dohner K, Krauter J, Frohling S, Corbacioglu A, Bullinger L, et al. Mutations and treatment outcome in cytogenetically normal acute myeloid leukemia. N Eng J Med. 2008;358:1909–18.
13. Jones PA, Baylin SB. The fundamental role of epigenetic events in cancer. Nat Rev Genet. 2002;3:415–28.
14. Esteller M, Fraga MF, Guo M, Garcia-Foncillas J, Hedenfalk I, Godwin AK, et al. DNA methylation patterns in hereditary human cancers mimic sporadic tumorigenesis. Hum Mol Genet. 2001;10:3001–7.
15. Galm O, Herman JG, Baylin SB. The fundamental role of epigenetics in hematopoietic malignancies. Blood Rev. 2006;20:1–13.
16. Herman JG. Hypermethylation of tumor suppressor genes in cancer. Semin Cancer Biol. 1999;9:359–67.
17. Esteller M, Corn PG, Baylin SB, Herman JG. A gene hypermethylation profile of human cancer. Cancer Res. 2001;61:3225–9.
18. Jones PA, Baylin SB. The epigenomics of cancer. Cell. 2007;128:683–92.
19. Figueroa ME, Abdel-Wahab O, Lu C, Ward PS, Patel J, Shih A, et al. Leukemic IDH1 and IDH2 mutations result in a hypermethylation phenotype, disrupt TET2 function, and impair hematopoietic differentiation. Cancer Cell. 2010;18:553–67.
20. Akalin A, Garrett-Bakelman FE, Kormaksson M, Busuttil J, Zhang L, Khrebtukova I, et al. Base-pair resolution DNA methylation sequencing reveals profoundly divergent epigenetic landscapes in acute myeloid leukemia. PLoS Genet. 2012;8: e1002781.
21. Cancer Genome Atlas Research Network. Genomic and epigenomic landscapes of adult de novo acute myeloid leukemia. N Eng J Med. 2013;368:2059–74.
22. Lugthart S, Figueroa ME, Bindels E, Skrabanek L, Valk PJ, Li Y, et al. Aberrant DNA hypermethylation signature in acute myeloid leukemia directed by EVI1. Blood. 2011;117:234–41.
23. Liu S, Shen T, Huynh L, Klisovic MI, Rush LJ, Ford JL, et al. Interplay of RUNX1/MTG8 and DNA methyltransferase 1 in acute myeloid leukemia. Cancer Res. 2005;65:1277–84.
24. Schoofs T, Berdel WE, Muller-Tidow C. Origins of aberrant DNA methylation in acute myeloid leukemia. Leukemia. 2014;28:1–14.
25. Schoofs T, Rohde C, Hebestreit K, Klein HU, Gollner S, Schulze I, et al. DNA methylation changes are a late event in acute promyelocytic leukemia and coincide with loss of transcription factor binding. Blood. 2013;121:178–87.
26. Gebhard C, Benner C, Ehrich M, Schwarzfischer L, Schilling E, Klug M, et al. General transcription factor binding at CpG islands in normal cells correlates with resistance to de novo DNA methylation in cancer cells. Cancer Res. 2010;70:1398–407.
27. Stadler MB, Murr R, Burger L, Ivanek R, Lienert F, Scholer A, et al. DNA-binding factors shape the mouse methylome at distal regulatory regions. Nature. 2011;480:490–5.
28. Metzeler KH, Becker H, Maharry K, Radmacher MD, Kohlschmidt J, Mrozek K, et al. ASXL1 mutations identify a high-risk subgroup of older patients with primary cytogenetically normal AML within the ELN Favorable genetic category. Blood. 2011;118:6920–9.
29. Feldman N, Gerson A, Fang J, Li E, Zhang Y, Shinkai Y, et al. G9a-mediated irreversible epigenetic inactivation of Oct-3/4 during early embryogenesis. Nat Cell Biol. 2006;8:188–94.
30. Tachibana M, Matsumura Y, Fukuda M, Kimura H, Shinkai Y. G9a/GLP complexes independently mediate H3K9 and DNA methylation to silence transcription. EMBO J. 2008;27:2681–90.
31. Ernst T, Chase AJ, Score J, Hidalgo-Curtis CE, Bryant C, Jones AV, et al. Inactivating mutations of the histone methyltransferase gene EZH2 in myeloid disorders. Nat Genet. 2010;42:722–6.
32. Shih AH, Abdel-Wahab O, Patel JP, Levine RL. The role of mutations in epigenetic regulators in myeloid malignancies. Nat Rev Cancer. 2012;12:599–612.
33. Delhommeau F, Dupont S, Della Valle V, James C, Trannoy S, Masse A, et al. Mutation in TET2 in myeloid cancers. N Eng J Med. 2009;360:2289–301.
34. Estecio MR, Issa JP. Tackling the methylome: recent methodological advances in genome-wide methylation profiling. Genome Med. 2009;1:106.
35. Esteller M. CpG island hypermethylation and tumor suppressor genes: a booming present, a brighter future. Oncogene. 2002;21:5427–40.
36. Schlesinger Y, Straussman R, Keshet I, Farkash S, Hecht M, Zimmerman J, et al. Polycomb-mediated methylation on Lys27 of histone H3 pre-marks genes for de novo methylation in cancer. Nat Genet. 2007;39:232–6.
37. Deneberg S, Guardiola P, Lennartsson A, Qu Y, Gaidzik V, Blanchet O, et al. Prognostic DNA methylation patterns in cytogenetically normal acute myeloid leukemia are predefined by stem cell chromatin marks. Blood. 2011;118:5573–82.
38. Dunwell T, Hesson L, Rauch TA, Wang L, Clark RE, Dallol A, et al. A genome-wide screen identifies frequently methylated genes in haematological and epithelial cancers. Mol Cancer. 2010;9:44.
39. Easwaran H, Johnstone SE, Van Neste L, Ohm J, Mosbruger T, Wang Q, et al. A DNA hypermethylation module for the stem/progenitor cell signature of cancer. Genome Res. 2012;22:837–49.
40. Pfirrmann M, Ehninger G, Thiede C, Bornhauser M, Kramer M, Rollig C, et al. Prediction of post-remission survival in acute myeloid leukaemia: a post-hoc analysis of the AML96 trial. Lancet Oncol. 2012;13:207–14.
41. Grassinger J, Simon M, Mueller G, Drewel D, Andreesen R, Hennemann B. Bone morphogenetic protein (BMP)-7 but not BMP-2 and BMP-4 improves maintenance of primitive peripheral blood-derived hematopoietic progenitor cells (HPC) cultured in serum-free medium supplemented with early acting cytokines. Cytokine. 2007;40:165–71.
42. Ehrich M, Nelson MR, Stanssens P, Zabeau M, Liloglou T, Xinarianos G, et al. Quantitative high-throughput analysis of DNA methylation patterns by base-specific cleavage and mass spectrometry. Proc Natl Acad Sci USA. 2005;102:15785–90.
43. Thiede C, Steudel C, Mohr B, Schaich M, Schakel U, Platzbecker U, et al. Analysis of FLT3-activating mutations in 979 patients with acute myelogenous leukemia: association with FAB subtypes and identification of subgroups with poor prognosis. Blood. 2002;99:4326–35.
44. Thiede C, Creutzig E, Illmer T, Schaich M, Heise V, Ehninger G, et al. Rapid and sensitive typing of NPM1 mutations using LNA-mediated PCR clamping. Leukemia. 2006;20:1897–9.
45. Rollig C, Bornhauser M, Kramer M, Thiede C, Ho AD, Kramer A, et al. Allogeneic stem-cell transplantation in patients with NPM1-mutated acute myeloid leukemia: results from a

prospective donor versus no-donor analysis of patients after upfront HLA typing within the SAL-AML 2003 trial. J Clin Oncol. 2015;33:403–10.
46. Damm F, Thol F, Hollink I, Zimmermann M, Reinhardt K, van den Heuvel-Eibrink MM, et al. Prevalence and prognostic value of IDH1 and IDH2 mutations in childhood AML: a study of the AML-BFM and DCOG study groups. Leukemia. 2011;25: 1704–10.
47. Gebhard C, Schwarzfischer L, Pham TH, Schilling E, Klug M, Andreesen R, et al. Genome-wide profiling of CpG methylation identifies novel targets of aberrant hypermethylation in myeloid leukemia. Cancer Res. 2006;66:6118–28.
48. Schmidl C, Klug M, Boeld TJ, Andreesen R, Hoffmann P, Edinger M, et.al. Lineage-specific DNA methylation in T cells correlates with histone methylation and enhancer activity. Genome Res. 2009; 2008;7:1165–74.
49. Schilling E, Rehli M. Global, comparative analysis of tissue-specific promoter CpG methylation. Genomics. 2007;90:314–23.
50. Freeman TC, Goldovsky L, Brosch M, van Dongen S, Maziere P, Grocock RJ, et al. Construction, visualisation, and clustering of transcription networks from microarray expression data. PLoS Comput Biol. 2007;3:2032–42.
51. Russler-Germain DA, Spencer DH, Young MA, Lamprecht TL, Miller CA, Fulton R, et al. The R882H DNMT3A mutation associated with AML dominantly inhibits wild-type DNMT3A by blocking its ability to form active tetramers. Cancer Cell. 2014;25:442–54.
52. Alvarez S, Suela J, Valencia A, Fernandez A, Wunderlich M, Agirre X, et al. DNA methylation profiles and their relationship with cytogenetic status in adult acute myeloid leukemia. PLoS ONE. 2010;5:e12197.
53. Bullinger L, Ehrich M, Dohner K, Schlenk RF, Dohner H, Nelson MR, et al. Quantitative DNA methylation predicts survival in adult acute myeloid leukemia. Blood. 2010;115:636–42.
54. Figueroa ME, Lugthart S, Li Y, Erpelinck-Verschueren C, Deng X, Christos PJ, et al. DNA methylation signatures identify biologically distinct subtypes in acute myeloid leukemia. Cancer Cell. 2010;17:13–27.
55. Bracken AP, Dietrich N, Pasini D, Hansen KH, Helin K. Genome-wide mapping of polycomb target genes unravels their roles in cell fate transitions. Genes Dev. 2006;20:1123–36.
56. Grubach L, Juhl-Christensen C, Rethmeier A, Olesen LH, Aggerholm A, Hokland P, et al. Gene expression profiling of Polycomb, Hox and Meis genes in patients with acute myeloid leukaemia. Eur J Haematol. 2008;81:112–22.
57. Ohm JE, McGarvey KM, Yu X, Cheng L, Schuebel KE, Cope L, et al. A stem cell-like chromatin pattern may predispose tumor suppressor genes to DNA hypermethylation and heritable silencing. Nat Genet. 2007;39:237–42.
58. Bracken AP, Helin K. Polycomb group proteins: navigators of lineage pathways led astray in cancer. Nat Rev Cancer. 2009;9:773–84.
59. Widschwendter M, Fiegl H, Egle D, Mueller-Holzner E, Spizzo G, Marth C, et al. Epigenetic stem cell signature in cancer. Nat Genet. 2007;39:157–8.
60. Vire E, Brenner C, Deplus R, Blanchon L, Fraga M, Didelot C, et al. The polycomb group protein EZH2 directly controls DNA methylation. Nature. 2006;439:871–4.
61. Wertheim GB, Smith C, Luskin M, Rager A, Figueroa ME, Carroll M, et al. Validation of DNA methylation to predict outcome in acute myeloid leukemia by use of xMELP. Clin Chem. 2015;61:249–58.
62. Taskesen E, Bullinger L, Corbacioglu A, Sanders MA, Erpelinck CA, Wouters BJ, et al. Prognostic impact, concurrent genetic mutations, and gene expression features of AML with CEBPA mutations in a cohort of 1182 cytogenetically normal AML patients: further evidence for CEBPA double mutant AML as a distinctive disease entity. Blood. 2011;117:2469–75.
63. Marcucci G, Maharry K, Radmacher MD, Mrozek K, Vukosavljevic T, Paschka P, et al. Prognostic significance of, and gene and microRNA expression signatures associated with, CEBPA mutations in cytogenetically normal acute myeloid leukemia with high-risk molecular features: a Cancer and Leukemia Group B Study. J Clin Oncol. 2008;26:5078–87.
64. Bienz M, Ludwig M, Leibundgut EO, Mueller BU, Ratschiller D, Solenthaler M, et al. Risk assessment in patients with acute myeloid leukemia and a normal karyotype. Cancer Res. 2005;11:1416–24.
65. Frohling S, Schlenk RF, Stolze I, Bihlmayr J, Benner A, Kreitmeier S, et al. CEBPA mutations in younger adults with acute myeloid leukemia and normal cytogenetics: prognostic relevance and analysis of cooperating mutations. J Clin Oncol. 2004;22:624–33.
66. Barjesteh van Waalwijk van Doorn-Khosrovani S, Erpelinck C, Meijer J, van Oosterhoud S, van Putten WL, Valk PJ, et al. Biallelic mutations in the CEBPA gene and low CEBPA expression levels as prognostic markers in intermediate-risk AML. Hematol J. 2003;4:31–40.
67. Preudhomme C, Sagot C, Boissel N, Cayuela JM, Tigaud I, de Botton S, et al. Favorable prognostic significance of CEBPA mutations in patients with de novo acute myeloid leukemia: a study from the Acute Leukemia French Association (ALFA). Blood. 2002;100:2717–23.
68. Shin SY, Lee ST, Kim HJ, Cho EH, Kim JW, Park S, et al. Mutation profiling of 19 candidate genes in acute myeloid leukemia suggests significance of DNMT3A mutations. Oncotarget. 2016;7:54825–37.
69. Wilop S, Fernandez AF, Jost E, Herman JG, Brummendorf TH, Esteller M, et al. Array-based DNA methylation profiling in acute myeloid leukaemia. Br J Haematol. 2011;155:65–72.
70. Figueroa ME, Wouters BJ, Skrabanek L, Glass J, Li Y, Erpelinck-Verschueren CA, et al. Genome-wide epigenetic analysis delineates a biologically distinct immature acute leukemia with myeloid/T-lymphoid features. Blood. 2009;113:2795–804.
71. Wouters BJ, Jorda MA, Keeshan K, Louwers I, Erpelinck-Verschueren CA, Tielemans D, et al. Distinct gene expression profiles of acute myeloid/T-lymphoid leukemia with silenced CEBPA and mutations in NOTCH1. Blood. 2007;110: 3706–14.